Evaluation of fracture strength of TiN thin films deposited on WC-Co substrate

T. Takamatsu[1], Y. Miyoshi[1], H. Tanabe[1], T. Itoh[2]

[1] The University of Shiga Prefecture, Japan
[2] NSK Ltd., Japan

Abstract

To evaluate the fracture strength of TiN thin films deposited on the hard metal substrate WC-Co, and to investigate the influence of the deposition conditions (bias voltage V_B) on the fracture strength of TiN thin films, the sphere indentation test was carried out to determine the ring crack initiation strength $s_{f,m}$ in TiN thin films deposited on two kinds of WC-Co substrates differing in hardness using sphere indenters of varying diameter. TiN thin films 2μm thick were deposited by dc magnetron sputtering under various V_B. Based on the probabilistic theory assuming a two-parameter Weibull distribution, the averages of the fracture strength s_f of TiN thin films without residual stress under conditions of uniform tensile stress and the residual stress s_R of thin films were predicted from the distribution characteristics of $s_{f,m}$. The main results were as follows: the average s_f is almost independent of sphere indenter and substrate hardness, and decreases with increasing V_B; the variation in s_f is mainly due to the grain size of thin films; the residual stress s_R increases with increasing V_B, and this tendency is qualitatively consistent with the measurements obtained by the X-ray diffraction method.

1. Introduction

Various coating technologies using ceramic thin films have been applied to allow use of cutting tools and machine components under more severe conditions. There have been many reports regarding the influence of coating conditions on the mechanical properties of thin films deposited on metal substrates, such as hardness, wear properties, and adhesion strength.

The deposition conditions are determined based on evaluation of the properties of thin films. However, a method for absolute evaluation of the fracture strength of thin films has not been established, and there have been few studies regarding the influence of deposition conditions on fracture strength of thin films.

Recently, we investigated the influence of deposition conditions on the mechanical properties of titanium nitride TiN thin films deposited on steel substrates by dc magnetron spattering [1]. The hardness of thin films and the adhesion strength clearly changed according to the deposition conditions, such as bias voltage V_B and gas pressure. The changes in mechanical properties of thin films can be explained based on the residual stress of thin films.

The present study was performed to investigate the validity of fracture strength evaluation of ceramic thin films deposited on hard metal substrates by a sphere indentation test method, and to clarify the influence of deposition conditions on the fracture strength of thin films. Furthermore, the validity of the prediction of residual stress on thin films from the results by the sphere indentation test was also examined.

1 Department of Mechanical Systems Engineering, The Univ. of Shiga Prefecture, 2500 Hassaka-cho, Hikone, Shiga 522-8533, Japan
2 1-6-3 Ohsaki, Shinagawa-Ku, Tokyo, Japan

2. Sphere Indentation Test

Figure 1 shows a schematic of the sphere indentation test. When a sphere indenter of a given diameter 2*R* is pressed on the thin film, a ring crack initiates on the thin film at a certain load. Ring cracks occur from micro-cracks in the thin film due to tensile stress in the radial direction slightly outside the region of contact.

Ichikawa *et al.* demonstrated that sphere indentation tests are effective for evaluation of the fracture strength of the surface layer in bulk ceramics [2]. Recently, we demonstrated the validity of sphere indentation tests to evaluate fracture toughness of micro-cracks in the surface layer of silicon nitride Si_3N_4 bulk material [3]. Furthermore, Ichikawa *et al.* reported that sphere indentation tests are possible to evaluate the fracture strength of thin films deposited on hard material substrates [4] [5].

In the previous study [6], we carried out sphere indentation tests using the tungsten-carbide WC-Co substrate with deposited alumina Al_2O_3 thin films and investigated the influence of the diameter of a sphere indenter, the hardness of substrate, and the thickness of thin films on the ring crack initiation strength of Al_2O_3 thin films.

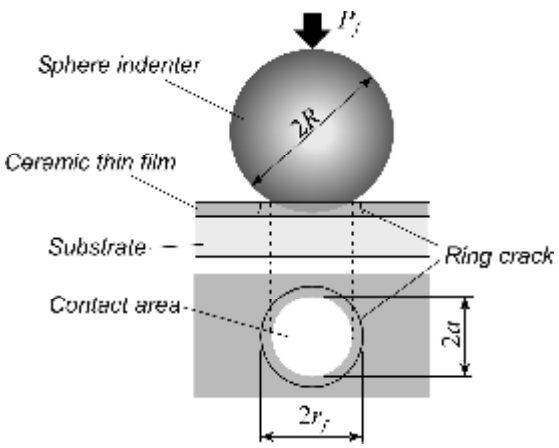

Figure 1: Schematic of sphere indentation test method

The ring crack initiation strength $\sigma_{f,m}$ of thin films was obtained by equation (1).

$$s_{f,m} = \frac{E_f\left(1+n_s\right)}{E_s\left(1+n_f\right)} \frac{(1-2n_s)P_f}{2p\, r_f^{\,2}} \quad (1)$$

E is Young's modulus, ν is Poisson's ratio, and *f* and *s* denote the thin film and the substrate, respectively. P_f is the ring crack initiation load, and r_f is the ring crack radius. This equation was introduced in approximation from Hertz's elastic contact theory based on the assumptions that both thin film and substrate show only elastic deformation, Young's modulus of a thin film is smaller than that of the substrate, and film thickness is sufficiently small compared with the contact circle radius [4].

As the average value of $\sigma_{f,m}$ is dependent on the diameter 2*R* of a spherical indenter, $s_{f,m}$ cannot be regarded as an absolute property of thin films. Therefore, based on the probabilistic theory assuming a two-parameter Weibull distribution, the distribution function of $\sigma_{f,m}$ was introduced in consideration of the residual stress of thin films [5].

3. Experimental Methods

Two types of WC-Co hard material were used as the substrate, the *F*-type and the *E*M-type. The Vickers hardness *HV* is 2050 for *F*-type and 1648 for *EM*-type. Three kinds of HIP-Si_3N_4 balls with diameters of 3.96, 5.95, and 7.93mm were used as sphere indenters. Young's modulus and Poisson's ratio of the substrate, sphere indenter, and TiN film are shown in Table 1.

Figure 2 shows the shape and dimensions of the specimen. The surface of 40×20mm^2 was finished using a diamond grinding stone (surface roughness *Ra*=0.05μm). TiN with film thickness

Tale 1: Mechanical properties of the material tested

Material	Indenter Si_3N_4	Substrate F-type WC-Co	Substrate EM-type WC-Co	Film TiN
Young's modulus GPa	304	610	550	415
Poison's ratio	0.28	0.3	0.3	0.19

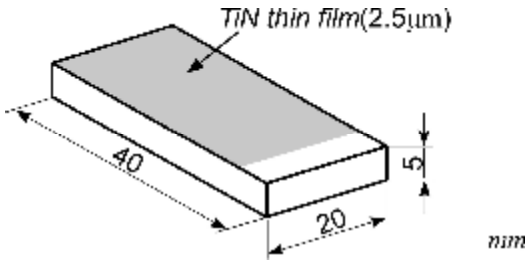

Figure 2: Shape and dimensions of the specimen.

Table 2: Deposition conditions of TiN thin film

Discharge current, A	2.21
Bias voltage V_B, V	0, -30, -60
Ar gas flow, ml/min	8.0
N_2 gas flow, ml/min	3.2
Thin Film thickness, μm	2.5

of about 2.5μm was deposited on the grinding surface using a dc magnetron sputtering equipment (Hirano Tecseed Co., Ltd.) as in the previous study [1].

Deposition conditions are shown in Table 2. Bias voltage V_B was 0V, –30V, or –60V. After deposition processing, the specimens were heated in a vacuum furnace for 30minutes at 400°C to improve the adhesion strength of thin films. TiN thin film hardness H_u was measured using an ultra-micro hardness testing machine (Mitutoyo Co., Ltd., MZT-3) and peel load was determined using a scratch testing machine (Rhesca Co., Ltd., CSR-01). The residual stress of the TiN thin film s_R was determined by X-ray stress measurement (Mac Science, Ltd., M03XHF^{22}). The microstructure of the thin film was observed using a scanning electron microscope (Hitachi, Ltd., S3000N).

Sphere indentation tests were carried out at a cross-head speed of 0.03~0.09mm/min using an Instron type testing machine (Tokyo Testing Machine Inc., SC-5M12). The ring crack initiation load P_f was determined using an AE analysis equipment (Showa Electric Laboratory Co., Ltd., SAS-5000). Applied load was interrupted at the load that detected AE by ring crack initiation, and load was unloaded at high speed. The contact area was observed using a digital microscope (Keyence Co., VH-8000); and data were considered valid when only a single ring crack was observed, and the diameter of the ring crack $2r_f$ measured. The distribution characteristics of $s_{f,m}$ on each specimen were obtained from many sphere indentation tests, changing the indentation position after each test. Furthermore, the apparent fracture toughness K_c^0 of thin films was evaluated using the same IF method as used for ceramic bulk material.

4. Experimental Results and Discussion

Figure 3 shows an example of a ring crack in the TiN thin film using $2R$=7.93mm. In the experiments in the present study, clear plastic. deformation was not observed on the substrate or the thin film at ring crack initiation.

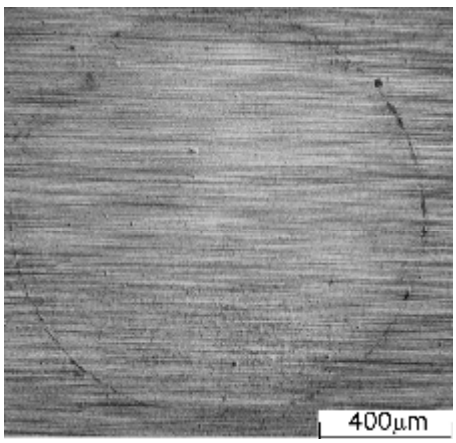

Figure 3: Example of a ring crack (F-type, $2R$=7.93mm, V_B=－60V)

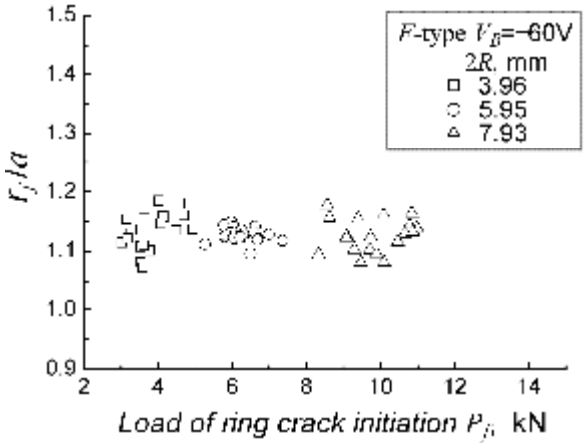

Figure 4: Relationship between r_f / a and P_f

Figure 4 shows the relationship between the ratio r_f/a and P_f for various 2R, where a is the contact circle radius and was obtained using equation (2):

$$a^3 = \frac{3}{4}R\left(\frac{1-n_b^2}{E_b}+\frac{1-n_s^2}{E_s}\right)P_f \quad (2)$$

R is the radius of the sphere indenter, and subscript b denotes the sphere indenter. Although equation (2) was obtained in Hertz's theory with a coating-less substrate, the equation is effective in approximation under conditions in which a is sufficiently large compared with film thickness. The values of r_f/a were almost constant and independent of P_f and 2R, although P_f varied widely with the diameter 2R. The average values of r_f/a were 1.08~1.20.

Figure 5 shows the ring crack initiation strength $s_{f,m}$ (2R=3.96 mm, V_B=−60 V) and the apparent fracture toughness $K_c^{\%}$ obtained from the IF method. The influence of substrate hardness on $K_c^{\%}$ is clear, but there was little influence on $s_{f,m}$. However, when plastic deformation of the substrate is large at ring crack initiation, $s_{f,m}$ will change with substrate hardness.

Figure 6 shows examples of the microstructure of the thin film of F-type substrate with V_B=0V

Figure 5: Comparison between IF-method and Sphere Indentation method

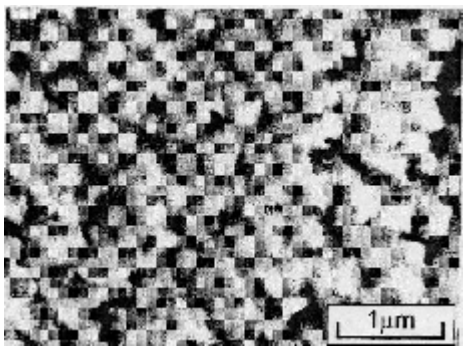

(a) V_B=0V

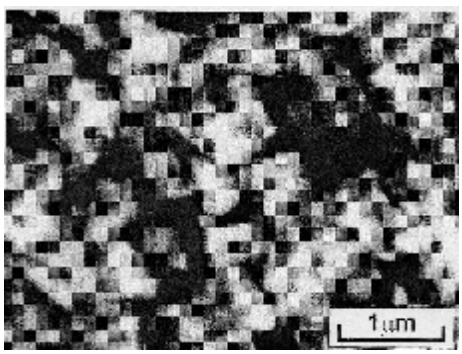

(b) V_B=−60V

Figure 6: Microstructure of thin films

and –60V. The crystal grain size increases with increasing bias voltage V_B, and the crystal direction also differs from V_B.

Figure 7 shows the relationship between the residual stress σ_R of thin films and the bias voltage V_B for both types of substrate. σ_R was determined by X-ray stress measurement.

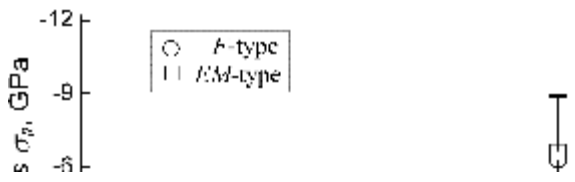

Figure 7: Relationship between σ_R and V_B (X-ray stress measurement)

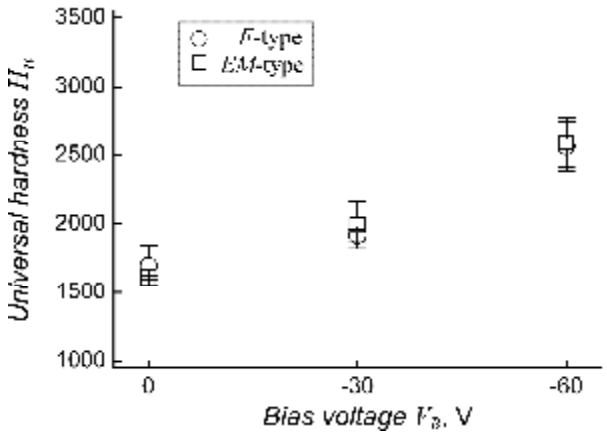

Figure 8: Relationship between H_u and V_B

Figure 8 shows the relationship between the hardness H_u of thin films and V_B for both types of substrate. The values of σ_R are almost 0 in the case of V_B=0V, and σ_R becomes compressive and increases with increasing V_B. The values of H_u increase similarly according to the increase in V_B. The above tendency of σ_R and H_u to V_B is the same as that reported previously. As described in the previous study [1], H_u is proportional to σ_R, *i.e.*, H_u is governed by σ_R. Although the scatter of adhesion strength was large, the adhesion strength did not clearly depend on V_B and the substrate hardness compared with that in H_u.

Figure 9 shows the Weibull probability of variations in ring crack initiation strength $s_{f,m}$ of

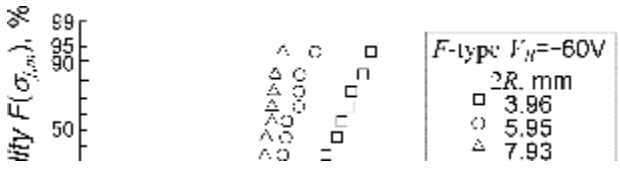

Fig.9 Variation of $s_{f,m}$ (Weibull probability Paper)

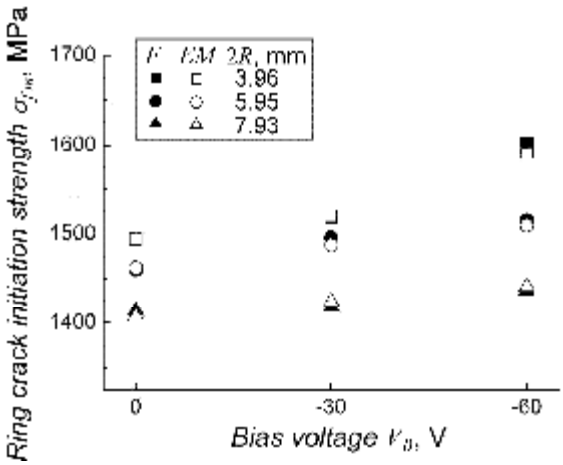

Figure 10: Relationship between $s_{f,m}$ and V_B

F-type substrate with different 2*R* in the case of V_B=−60V. It can be seen that $s_{f,m}$ nearly conforms to a two-parameter Weibull distribution, and that $s_{f,m}$ depends on 2*R*. The same result was obtained in the case of the *EM*-type substrate.

Figure 10 shows the relationship between the average $s_{f,m}$ and V_B in both substrates. The values of $s_{f,m}$ for both substrates increase with increasing V_B. The variation in $s_{f,m}$ is considered to be due to the residual stress s_R and the microstructure of thin films. The increasing tendency of $s_{f,m}$ cannot be explained from the changes in crystal grain size shown in Fig.6. That is, the tendency of $s_{f,m}$ mentioned in Fig.10 is thought to be mainly due to the change in s_R, as shown in Fig.7.

Ichikawa *et al.* introduced equation (3) of the distribution-function $F(s_{f,m})$ obtained based on the probabilistic theory (concept of the effective area) assuming a two-parameter Weibull distribution [5].

$$F(s_{f,m}) = 1 - \exp\left[\int_{r_f}^{r'} \left\{ \frac{\pi g^3 K^2}{a} \left(\frac{s_{f,m}}{r^2} - s_R \right) \right\}^{m_o} \frac{2\pi r}{A_o} dr \right] \quad (3)$$

Here, it was assumed that the residual stress s_R of thin films is uniform. m_o and h_o are the shape parameter and scale parameter of $s_{f,m}$ for a standard area A_o (=1.0mm^2) under conditions of uniform tensile stress and s_R=0. r is the distance from the center of the contact circle. a, g, and K are expressed according to the following equation.

$$a = \frac{E_f(1+n_s)}{E_s(1+n_f)} \qquad g = \frac{r_f}{a}$$

$$K = \frac{3\pi}{2}\left(\frac{1-n_b^2}{E_b} + \frac{1-n_s^2}{E_s} \right) \frac{R}{1-2n_s} \quad (4)$$

The integration range in equation (3) is from $r=r_f$ to $r=r'$ where the tensile stress in the radial direction on the surface of the film is almost zero.

In the case of V_B=0, the relationship between the average values of $s_{f,m}$ and the diameter 2R of a sphere indenter was predicted on the assumption of s_R=0. That is, in the case of s_R=0, integration of equation (3) can be calculated directly, and m_o and h_o are obtained from the following equations.

$$m_o = m - 2$$

$$h_o = \left\{ \frac{\pi g^6 K^2}{(m_o - 1)a^2 A_o} (5) h^{m_o+2} \right\}^{\frac{1}{m_o}}$$

Therefore, in the present study, m_o and h_o were determined using equation (5) from the distribution properties of $s_{f,m}$ with 2R=3.96mm (m, h).

Figure 11 shows the relationship between the average $s_{f,m}$ and 2R. The symbols ⊥ indicate the average and standard deviation of experimental values of F-type substrate, and the dotted line shows the predicted relationship. As shown in the figure, the predicted relationship and the experiments are almost in agreement. That is, the prediction of the $s_{f,m}$–2R relationship in the case of V_B=0 using equation (3) is effective.

Then, the fracture strength σ_f of thin films under a uniform tensile stress field without residual stress of thin films and the residual stress σ_R of thin films were predicted from the distribution properties of $s_{f,m}$ based on the probabilistic theory, assuming a two-parameter Weibull distribution. The averages of σ_f were calculated using m_o and h_o for each V_B.

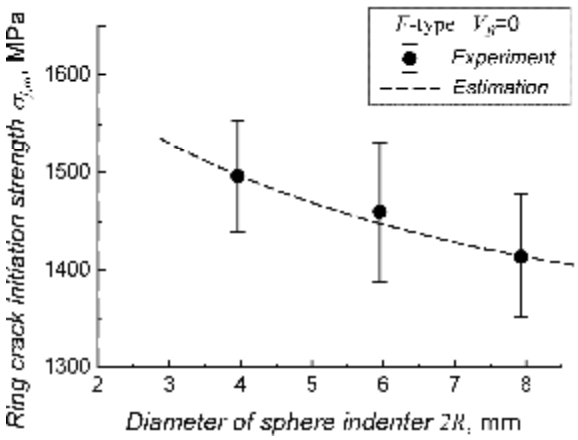

Figure 11: Relationship between $s_{f,m}$ and 2R

Figure 12 shows the relationship between average σ_f and V_B. As shown in the figure, σ_f tends to decrease with increases in V_B. This tendency of σ_f in relation to V_B is the opposite of that of $s_{f,m}$ shown in Fig.10. Although the influence of

crystal direction in the microstructure described in Fig.6 is unknown, the decreasing tendency of $\bar{\sigma}_f$ is considered mainly due to changes in the crystal grain size. In comparison with $s_{f,m}$ shown in Fig.10, the dependence of $\bar{\sigma}_f$ on $2R$ is small. That is, $\bar{\sigma}_f$ is considered an absolute evaluation value.

Figure 13 shows the relationship between the prediction of the residual stress $\bar{\sigma}_R$ of thin films and V_B. It can be seen that the value of $\bar{\sigma}_R$

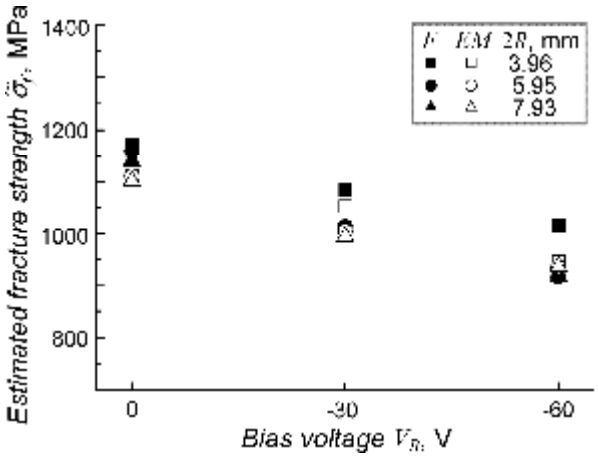

Figure 12: Relationship between $\bar{\sigma}_f$ and V_B

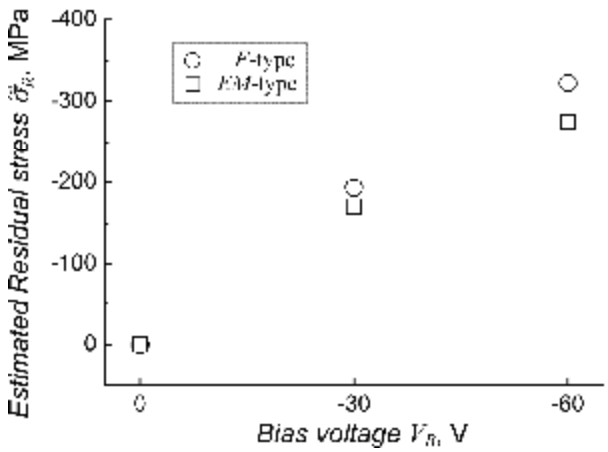

Figure 13: Relationship between $\bar{\sigma}_R$ and V_B

increases with increasing V_B, and this tendency is in agreement with that determined by X-ray stress measurement as shown in Fig.7. However, the values of $\bar{\sigma}_R$ are considerably smaller than those obtained by X-ray stress measurements. Equation (1) is an approximation, and the residual stress in thin films is not uniform but changes. That is, the results of recent studies [7][8] indicated that the residual stress near the surface is smaller than that on the inside. Further studies are required to evaluate the residual stress of thin films based on the results of sphere indentation tests.

5. Conclusions

To estimate the fracture strength of TiN thin films deposited on WC-Co substrates, to investigate the influence of the deposition conditions on the fracture strength of thin films, and to predict the residual stress of thin films from the distribution characteristics of the ring crack initiation strength of thin films, sphere indentation tests were carried out using two types of WC-Co substrate differing in hardness using sphere indenters of varying diameter. TiN thin film was deposited by dc magnetron sputtering under various V_B. The following conclusions were obtained.

- There is little influence of substrate hardness on the ring crack initiation strength $s_{f,m}$ of thin films, but apparent fracture toughness $\bar{K}_c$ determined by the IF-method is clearly dependent on the substrate hardness.

- The residual stress s_R of thin films measured by the X-ray diffraction method and the hardness H_u of thin films increase with increasing bias voltage V_B regardless of the substrate hardness. The crystal grain size also shows a tendency to increase with increasing V_B.

- The scatter of $s_{f,m}$ nearly conforms to a two-parameter Weibull distribution and the average $s_{f,m}$ is dependent on the diameter of a sphere indenter $2R$ regardless of V_B and substrate hardness.

- The value of $s_{f,m}$ increases with increasing V_B. This variation in $s_{f,m}$ is due to the changes in s_R of thin films.

- The relationship between the average $s_{f,m}$ and $2R$ can be predicted from the distribution properties of $s_{f,m}$ based on the probabilistic theory assuming a two-parameter Weibull distribution.

- The residual stress σ_R predicted from the distribution properties of $s_{f,m}$ is considerably smaller than that of X-ray stress measurement, but the prediction of the s_R–V_B relationship is quantitatively in agreement with that of X-ray stress measurement.

- The average fracture strength of thin film σ_f predicted from the distribution properties of $s_{f,m}$ under a uniform stress field and without the residual stress of thin film is almost independent of $2R$. Therefore, the sphere indentation test method is effective to evaluate the absolute fracture strength of thin films.

- The fracture strength of thin film σ_f decreases according to increases in V_B. The tendency of σ_f increase is mainly due to the crystal grain size of thin films.

6. References

[1] Tanabe, H., Miyoshi, Y., Takamatsu, T., Sugiura, H., *Journal of the Society of Materials Science, Japan*, Vol.51, No.6, pp.694-700, 2002(in Japanese) .

[2] Ichikawa, H., Ohogushi, K., Takamatsu, T., *Transactions of the Japan Society of Mechanical Engineers, Series A*, Vol.60, No.575, pp.1538-1544, 1994(in Japanese).

[3] Takamatsu, T., Miyoshi, Y., Tanabe, H., Segawa, M., *Transactions of the Japan Society of Mechanical Engineers, Series A*, Vol.71, No.708, pp.1147-1152, 2005(in Japanese).

[4] Kagawa, H., Ichikawa, H., Takamatsu, T., Kuwano, H., *Transactions of the Japan Society of Mechanical Engineers, Series A*,Vol.60, No.570, pp.416-420, 1994(in Japanes) .

[5] Kagawa, H., Ichikawa, H., Takamatsu, T., Kuwano, H., *Transactions of the Japan Society of Mechanical Engineers, Series A*, Vol.60, No.570, pp.396-401, 1994(in Japanese) .

[6] Takamatsu, T., Ichikawa, H., Matsumura, T., Kawasaki,T., *Journal of the Society of Materials Science, Japan*, Vol.47, No.8, pp.819-824, 1998(in Japanese).

[7] Tanaka, K, Akiba, Y., Kawai, M., Itho, T., *Journal of the Society of Materials Science, Japan*, Vol.54, No.7, pp.704-709, 2005(in Japanese).

[8] Takago, S., Yasui, H., Kuritsu, K., Sasaki, T., Hirose, S., Sakurai, K., BUNSEKI KAGAKU, Vol.55, No.6, pp.405-410, 2006(in Japanese).